

Stereospecific Synthesis of Enantiopure [6]Helicene Containing a Seven-Membered Ring and [7]Helicene through Acid-Promoted Stepwise Alkyne Annulations of Doubly Axial-Chiral Precursors

Tomoyuki Ikai,^{*[a],[b]} Kosuke Oki,^[a] Shoya Yamakawa,^[a] and Eiji Yashima^{*[a]}

[a] Dr. T. Ikai, Dr. K. Oki, S. Yamakawa, Prof. E. Yashima
Department of Molecular and Macromolecular Chemistry
Graduate School of Engineering, Nagoya University
Chikusa-ku, Nagoya 464-8603 (Japan)
E-mail: ikai@chembio.nagoya-u.ac.jp; yashima@chembio.nagoya-u.ac.jp

[b] Dr. T. Ikai
Precursory Research for Embryonic Science and Technology (PRESTO)
Japan Science and Technology Agency (JST)
Kawaguchi, Saitama 332-0012 (Japan)

Supporting information for this article is given via a link at the end of the document.

Abstract: The enantiopure seven-membered ring embedded [6]helicene and carbo[7]helicene (>99% ee) with an opposite helicity were simultaneously and quantitatively (>99%) synthesized with a perfect stereospecificity through stepwise acid-promoted intramolecular alkyne annulations of doubly axial-chiral cyclization precursors. The helical handedness of the [6]- and [7]helicenes was fully stereo-controlled by the doubly axial chirality of the precursors as a result of complete axial-to-helical chirality transfer. The cyclizations proceeded in a stepwise manner; the first six-membered ring formation was followed by the kinetically-controlled seven- or six-membered ring formation with or without helix-inversion of a [4]helicene intermediate generated during the first cyclization step, thus quantitatively producing enantiopure circularly polarized luminescent [6]- and [7]helicenes with an opposite helicity, respectively.

Spiral-shaped fully π -conjugated helicenes^[1] with a one-handed helical topology show significant optical rotations and unique chiroptical properties.^[2] Hence, enantiopure helicenes have been extensively applied as promising chiral materials for nonlinear optics,^[1f,g,3] chiral-induced spin selectivity,^[4] and circularly polarized luminescence (CPL)^[2f,5] as well as for asymmetric catalysis,^[6] etc. To date, structurally diverse optically-active carbohelicenes and their analogues including heterohelicenes^[1g,2d,e,f] have been synthesized in a highly enantio- and/or diastereoselective manner through catalytic asymmetric reactions using chiral metal- and organocatalysts^[1c,e,7] and stereospecific reactions of optically-active starting materials with point, axial, or planar chiralities.^[1c,e,8] Among them, the axially chiral biaryl derivatives have frequently been utilized as a powerful chiral auxiliary to control the helical geometry and handedness of the resulting carbo- and heterohelicenes since 1972 (Figure 1a).^[9,10] However, it remains a synthetic challenge to achieve both quantitative yields (>99%) and a perfect enantioselectivity (>99% enantiomeric excess (ee)). Thus, the development of a new and versatile synthetic approach to quantitatively produce enantiopure helicenes is highly desirable.

We now report the quantitative, stereospecific, and simultaneous synthesis of two enantiopure helicenes with an

opposite helicity, namely, (*P*)- or (*M*)-[6]helicene (**2**) containing a unique seven-membered ring^[11,12] and (*M*)- or (*P*)-[7]helicene (**3**), respectively, through acid-promoted stepwise alkyne annulations^[13,14] of optically-pure biaryl cyclization precursors with two axial chiralities ((*S,S*)-**1** and (*R,R*)-**1**). We found that the helical handedness of the [6]- and [7]helicenes was fully stereo-controlled by the doubly axial chirality of the precursors as a result of a complete axial-to-helical chirality transfer (Figure 1b). The mechanism of the simultaneous formations of the enantiopure [6]- and [7]helicenes and a unique seven-membered ring formation embedded in the [6]helicene framework as well as their circular dichroism (CD) and CPL activities were investigated.

The cyclization precursor, the 5,6-di(1-naphthyl)benzene derivative (**1**) containing 2-(4-alkoxy-2,6-dimethylphenyl)ethynyl pendants at the 1,4-positions of the central benzene ring, was synthesized according to Scheme S1 as a mixture of *racemo*-(*R,R*)/(*S,S*) and *meso*-(*S,R*) diastereomers ([*racemo*-**1**]/[*meso*-**1**] = 76 / 24) due to two axial chiralities arising from the tri-*ortho*-substituted biaryl structures, thus showing a complicated ¹H NMR spectrum (Figure S1a). The three stereoisomers were successfully isolated by chiral HPLC on a CHIRALPAK IA column (Daicel, Osaka, Japan) (Figure S1b–e). The first- and third-eluted isomers showed mirror image CDs, while the second-eluted isomer was CD silent (Figure S1f). Based on the observed and calculated CD spectra of the first-eluted isomer based on the time-dependent-density functional theory (TD-DFT) (Figure S4b) along with its structure determined by single-crystal X-ray crystallography (Figures 4c and S4a), the first-, second-, and third-eluted stereoisomers were assigned as (*S,S*)-, (*S,R*)-, and (*R,R*)-**1**, respectively (Figure S1b–e). The optical activity of (*S,S*)-**1** remained unchanged in toluene at 100 °C after 12 h (Figure S5), indicating the static biaryl axial chirality of **1**.

The trifluoroacetic acid (TFA)-promoted alkyne annulations of the isolated enantiopure (*S,S*)- and (*R,R*)-**1** with >99% ee and *meso*-(*S,R*)-**1** were then performed in dichloromethane at room temperature according to a previously reported method (Scheme S2 and Figures 2a, S6a, S7, and S8a),^[14] which were completed within 10 h as confirmed by IR analysis (Figure S9b,e,h). We anticipated the exclusive formation of either a right- (*P*) or left-

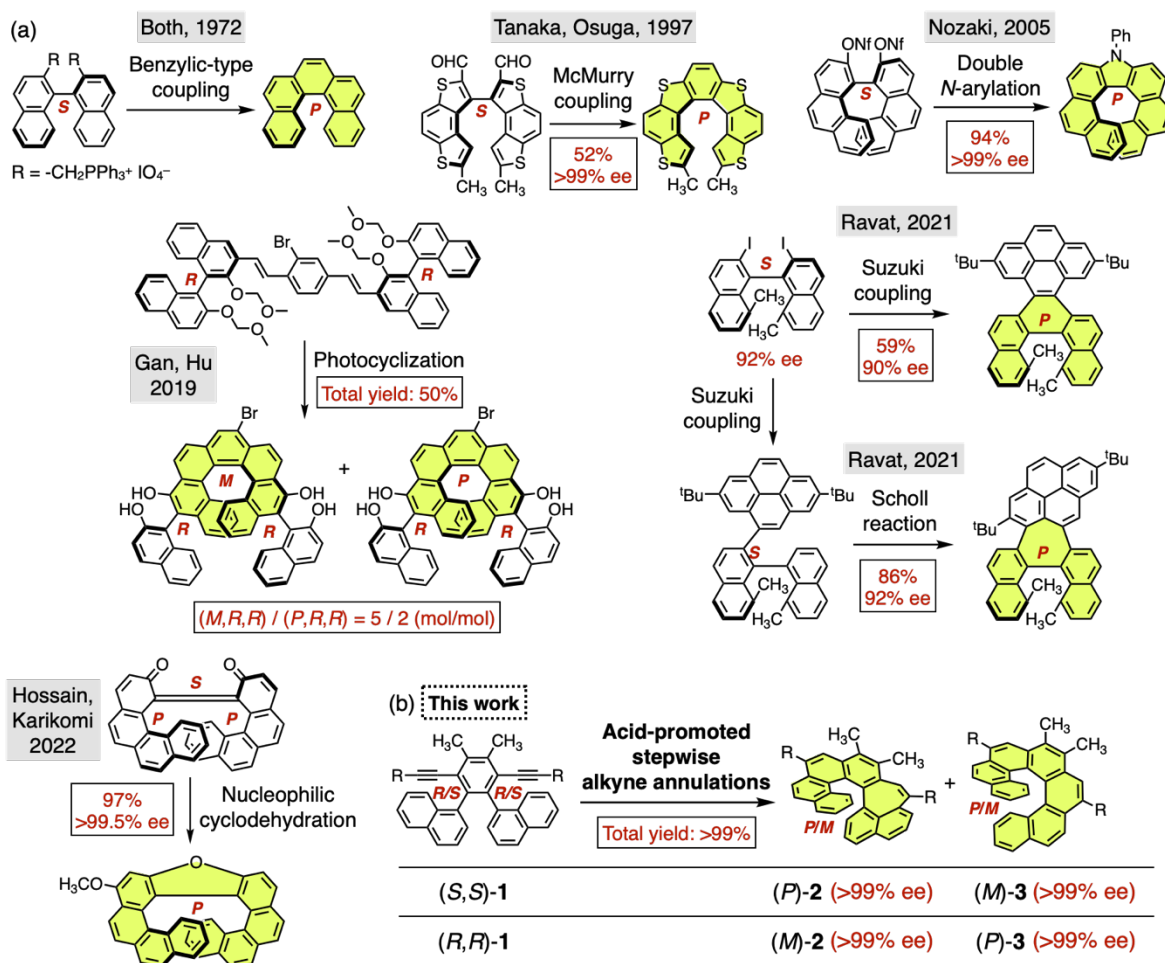


Figure 1. (a) Representative examples of the synthesis of optically-active carbo- and heterohelicenes through stereospecific reactions of optically-active cyclization precursors with an axial chirality. (b) Quantitative, stereospecific, and simultaneous formations of the enantiopure [6]helicene (**2**) containing a seven-membered ring and [7]helicene (**3**) through acid-promoted stepwise alkyne annulations of an optically-pure cyclization precursor ((S,S)- or (R,R)-1) with two axial chiralities.

(M) handed [7]helicene or its racemic mixture, but the ¹H NMR spectra of the cyclization products were complicated with a similar signal pattern (Figures S6a, S7, and S8a), indicative of the formation of multiple products. A product mixture obtained from the *meso*-(S,R)-1 as well as that produced from the *racemo*-1 (*racemo*-1/*meso*-1 = 76/24) was resolved into two pairs of peaks (f1/f4 and f2/f3 fractions) by chiral HPLC with dual UV and CD detectors (Figures S8b and S10a). Interestingly, each isolated pair exhibited the perfect mirror image CDs, indicating the formation of two pairs of enantiomers (**2** and **3**) (Figures S10f,g and 5a,b). The structures of *rac*-**2** and *rac*-**3** corresponding to the f1/f4 and f2/f3 fractions were unambiguously determined by single-crystal X-ray crystallography, which revealed the simultaneous formation of a unique [6]helicene ((P)/(M)-**2**) composed of one seven-membered ring (Figure 3a,c)^[12] as well as the expected [7]helicene ((P)/(M)-**3**) (Figure 3b,d), as supported by 1D and 2D NMR and high-resolution mass analyses (Figures 2c,d, S11, and S12). Based on the comparison between the observed and calculated CD spectra (Figures S13b and S14b), the four stereoisomers (f1–f4) in Figures 2b, S8b, and S10 were definitely identified as (P)-**2**, (P)-**3**, (M)-**3**, and (M)-**2**, respectively.

As a result, the biaryl axially chiral (S,S)- and (R,R)-1 were found to be quantitatively converted into two enantiopure [6]- and [7]-helicenes (>99% ee) [(P)-**2** and (M)-**3**] and [(M)-**2** and (P)-**3**], respectively, in a perfect enantioselective manner through

modified acid-promoted alkyne annulations (Figure 2a). Although a number of stereospecific syntheses of optically-active helicenes has been reported,^[9,10] to the best of our knowledge, this is the first example of the quantitative, stereospecific, and simultaneous synthesis of two enantiopure helicenes from a single enantiopure precursor through a versatile acid-promoted alkyne annulation, which totally relies on a complete axial-to-helical chirality transfer (Figure 1b).

The nucleus-independent chemical shifts (NICS)^[15] were calculated to investigate the local aromaticity of the individual six- and/or seven-membered rings of **2** and **3**. The aromatic character of all the six-membered rings in **2** and **3** was confirmed by their negative NICS(0) and NICS(1) values in the ranges of -11.1 to -3.8 and -13.2 to -7.1, respectively (Figure 3a,b), while the seven-membered ring (E) in **2** shows high positive NICS(0) (+8.7) and NICS(1) (+4.8) values (Figure 3a), indicating its nonaromatic character, as observed in the previously reported helicenes embedded with a seven-membered ring.^[9h,i,12c-e]

We propose a plausible mechanism for the simultaneous formations of the enantiopure seven-membered ring-embedded [6]helicene (**2**) and carbo[7]helicene (**3**) with an opposite helicity during the acid-promoted alkyne annulations of (S,S)- and (R,R)-1, which takes place in an enantioselective stepwise manner, namely, the first six-membered ring formation followed by the six- or seven-membered ring formation, thereby producing the

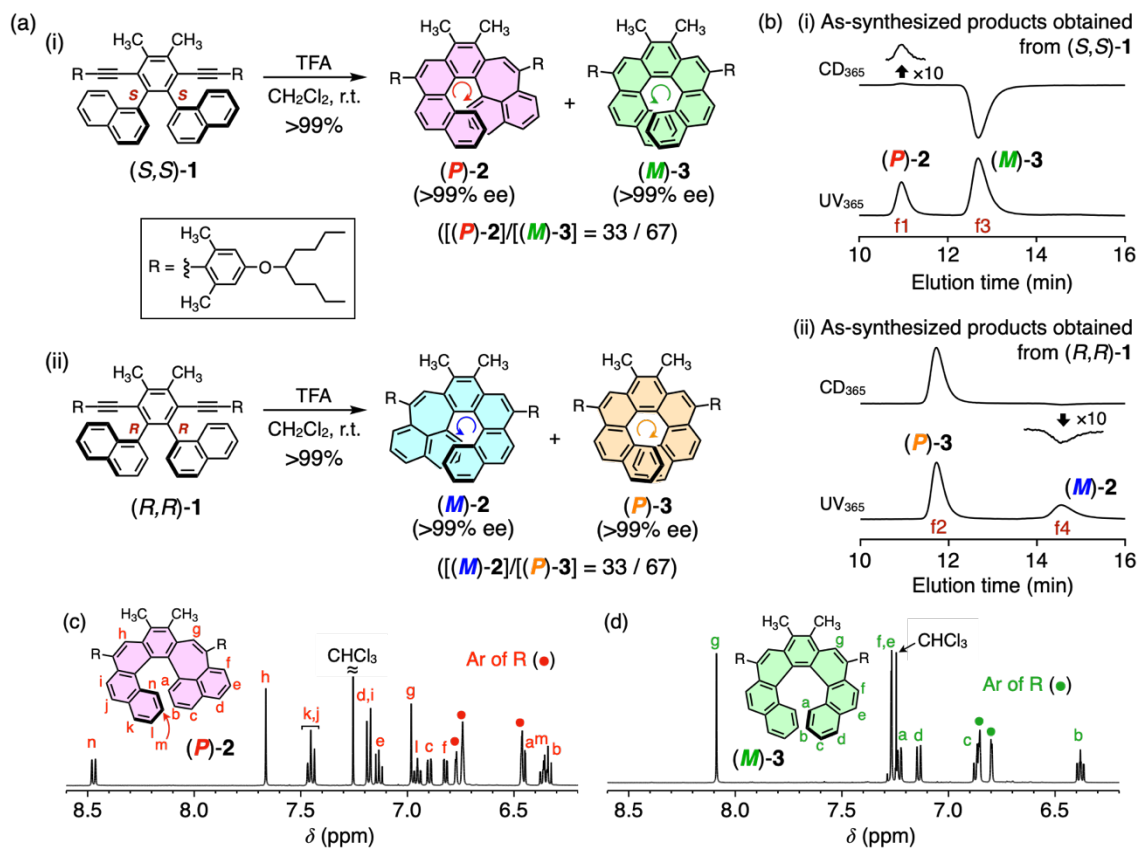


Figure 2. (a) Quantitative, stereospecific, and simultaneous formations of enantiopure [(*P*)-2 and (*M*)-3] and [(*M*)-2 and (*P*)-3] helicenes through acid-promoted stepwise alkyne annulations of axially-chiral (*S,S*)-1 (i) and (*R,R*)-1 (ii), respectively. For the formations of racemic mixtures of 2 and 3 helicenes from *meso*-1 ((*S,R*)-1), see Figure S8. (b) Chiral HPLC chromatograms (dual UV and CD detectors set at 365 nm) of as-synthesized cyclization products obtained from (*S,S*)-1 (i) and (*R,R*)-1 (ii). Chromatographic conditions: column, CHIRALPAK IA (0.46 cm (i.d.) × 25 cm) and CHIRALPAK IB N-5 (0.46 cm (i.d.) × 25 cm) connected in series; eluent, *n*-hexane/dichloromethane (99/1, v/v); flow rate, 1.0 mL min⁻¹; temperature, 25 °C. For the fraction numbers (f1–f4), see Figure S10. (c,d) 1H NMR spectra (500 MHz, $CDCl_3$, 25 °C) of the isolated (*P*)-2 (c) and (*M*)-3 (d). For the signal assignments, see the Supporting Information, Figures S11 and S12. The absolute configurations were assigned based on the TD-DFT calculations (Figures S13b and S14b).

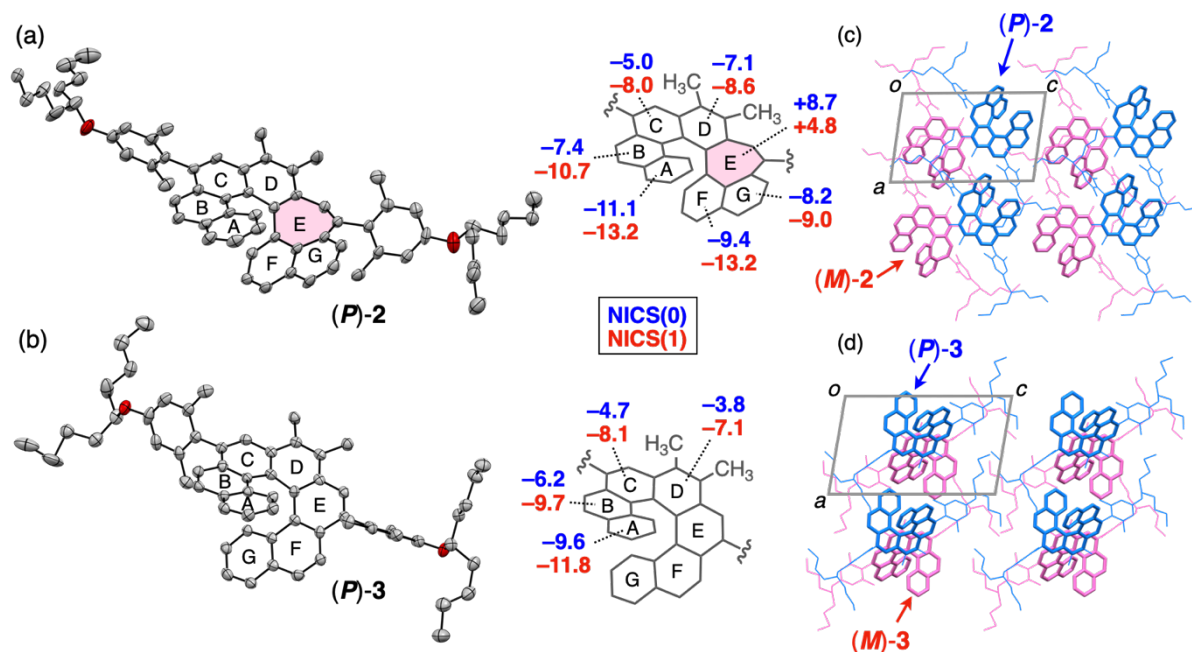


Figure 3. (a,b) Perspective views of the crystal structures of *rac*-2 (a) and *rac*-3 (b) with thermal ellipsoids at 50% probability. The NICS(0) and NICS(1) values of each ring of the helicene backbones calculated at the GIAO-HF/6-311G(d,p) level for the geometry-optimized structures (see Figures S13a and S14a) are highlighted in blue and red, respectively. (c,d) Crystal packing structures of (*P*)/(*M*)-2 (c) and -3 (d) as viewed along the *b* axis of the unit cell shown in gray. The helicene backbones and the 4-alkoxy-2,6-dimethylphenyl pendant groups are represented by capped-stick and wireframe models, respectively, and (*P*)- and (*M*)-helicene frameworks of 2 and -3 are colored in blue and pink, respectively. All the hydrogen atoms, solvent molecules, and disordered atoms are omitted for clarity.

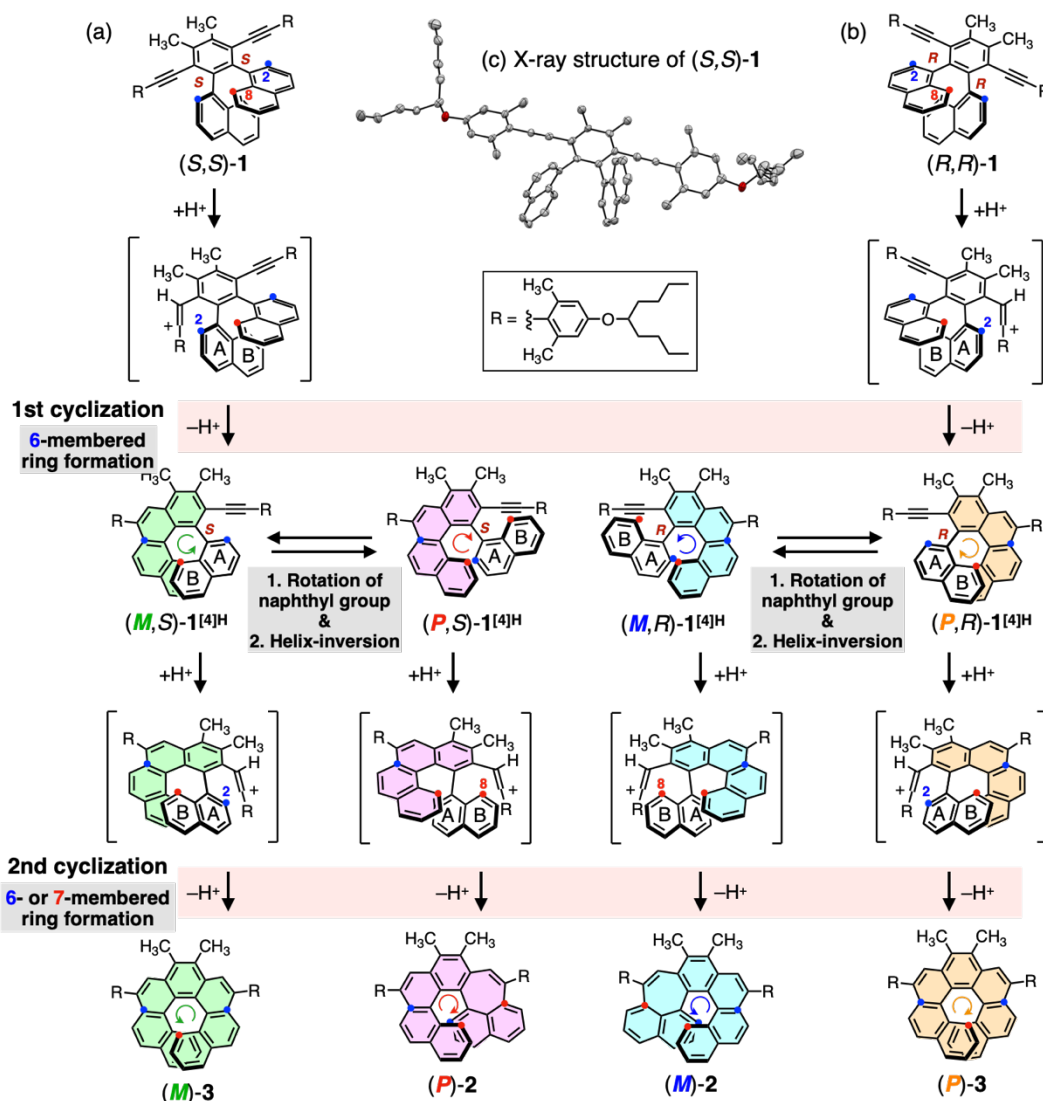


Figure 4. Plausible mechanism for the stereospecific simultaneous formations of [6]helicene (**2**) containing a seven-membered ring and [7]helicene (**3**) through the acid-promoted stepwise alkyne annulations of (S,S) -**1** (a) and (R,R) -**1** (b), which involve the first six-membered ring formation followed by the six- or seven-membered ring formation. The reacting carbon atoms at the 2- and 8-positions of the naphthalene rings are highlighted in blue and red circles, respectively. For the formation mechanism of racemic mixtures of **2** and **3** helicenes from *meso*-(S,R)-**1**, see Figure S15. (c) Perspective view of the crystal structure of (S,S) -**1** with thermal ellipsoids at 50% probability.

enantiopure [7]- (**3**) and seven-membered ring-embedded [6]- (**2**) helicenes, respectively. The unique seven-membered ring formation is accompanied by inversion of a [4]helicene intermediate during the second cyclization process, thus producing the opposite-handed [6]helicene (**2**) (Figure 4).

For example, when (S,S) -**1** is treated with TFA, the first acid-catalyzed electrophilic intramolecular cyclization occurs at the 2-position of either naphthyl unit (ring A) with the close vinyl carbocation formed through protonation of one of the ethynyl groups,^[14] thus forming an intermediate with the (M) -[4]helicene framework ((M,S) -**1**^{[4]H}). Subsequent intramolecular cyclization at the same 2-position of the other naphthyl unit (ring A) results in the formation of the expected [7]helicene (M) -**3** through fully six-member ring formations (Figure 4a, left). We postulate that an equilibrium exists in the (M) -[4]helicene intermediate ((M,S) -**1**^{[4]H}), which can be converted to its diastereomer (P,S) -**1**^{[4]H} with the opposite (P) -[4]helicene chirality by rotation of the naphthyl ring, while maintaining its biaryl (S)-axial chirality. If this is the case, as schematically illustrated in Figure 4a (right), the 8-position of the naphthyl unit (ring B) of (P,S) -**1**^{[4]H} is positioned close to the vinyl

carbocation. Hence, the second electrophilic intramolecular cyclization of (P,S) -**1**^{[4]H} proceeds to give (P) -**2** composed of an unexpected seven-membered ring. Alcarazo et al.^[16] reported the highly-enantioselective catalytic synthesis of carbo[6]helicenes through similar sequential alkyne annulations of achiral diynes catalyzed by chiral Au-complexes. Later, Yan et al.^[17] developed an elegant approach to control both the helical and axial chirality of binaphthyl-containing [6]helicenes during the enantio- and diastereoselective stepwise alkyne annulations of achiral diynes catalyzed by chiral basic organocatalysts.^[18]

At low temperatures, such an interconvertible diastereomeric conformational equilibrium is expected to shift to either (M,S) -**1**^{[4]H} or (P,S) -**1**^{[4]H}. In fact, the alkyne annulations of (S,S) - and (S,R) -**1** with TFA in dichloromethane at -20 °C yielded a mixture of [(P) -**2** and (M) -**3**] and [*rac*-**2** and *rac*-**3**] at the ratios of 24:76 and 62:38 (Figures S6b and S8c), respectively, which were different from those produced at room temperature (33:67 and 51:49, respectively) (Figures S6a and S8a). At -20 °C, the rotation of the naphthyl group of the [4]helicene intermediates (**1**^{[4]H}) derived from (S,S) - and (S,R) -**1** is likely suppressed (Figures 4a and S15),

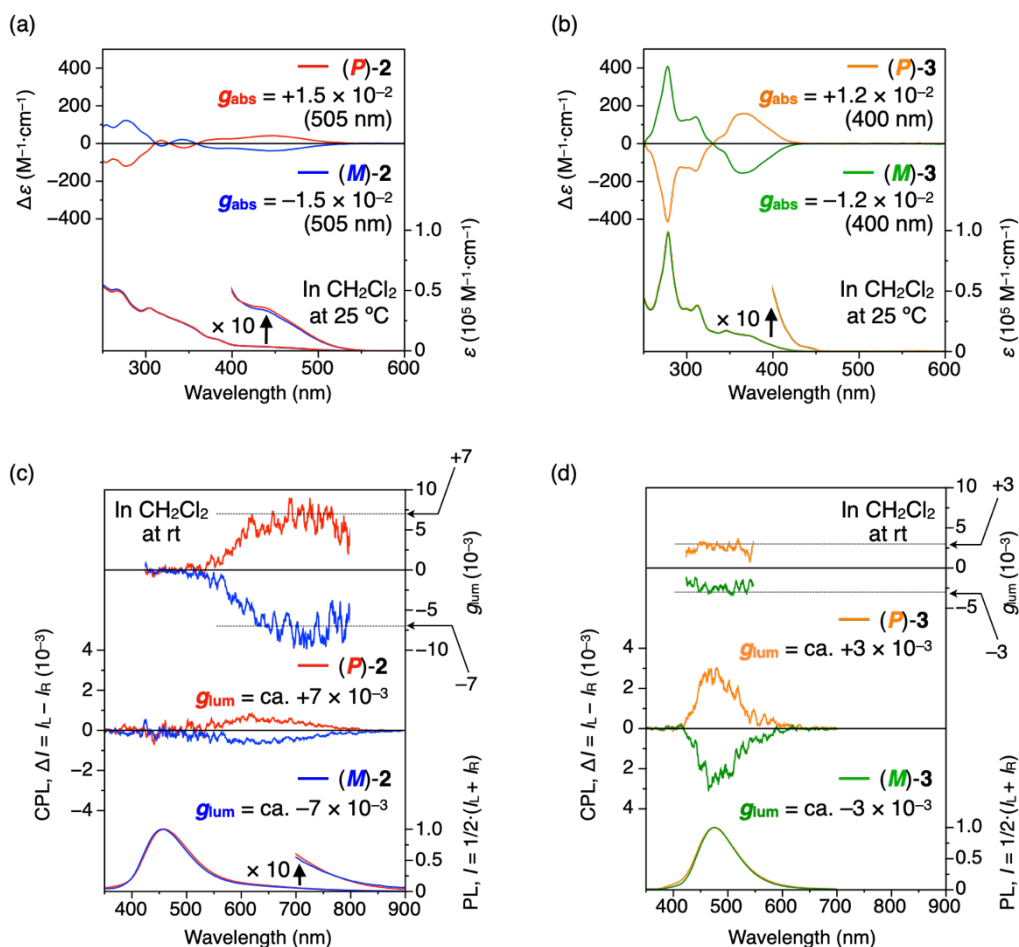


Figure 5. (a,b) CD and absorption spectra of (*P*)- and (*M*)-**2** (a) and (*P*)- and (*M*)-**3** (b) in dichloromethane at 25 °C. Maximum Kuhn's dissymmetry factors ($g_{\text{abs}} = \Delta\epsilon/\epsilon$) are also shown. [Helicene] = ca. 1×10^{-4} M. (c,d) Normalized PL (bottom), CPL (middle), and g_{lum} (top) spectra of (*P*)- and (*M*)-**2** (c) and (*P*)- and (*M*)-**3** (d) in dichloromethane at room temperature. The g_{lum} values are defined as $2(I_L - I_R)/(I_L + I_R)$, where I_L and I_R are the PL intensities of the left- and right-handed circularly polarized light, respectively. $\lambda_{\text{ex}} = 300$ nm. [Helicene] = ca. 2×10^{-5} M.

thereby enhancing the chemoselectivity under kinetic control. These results further support the proposed stepwise double cyclization mechanism that involves helix-inversion of the [4]helicene intermediates formed after the first six-membered ring formation (Figures 4 and S15).

According to this mechanism, when (*R,R*)-**1** and (*S,R*)-**1** are used as cyclization precursors, the formations of the enantiopure (*M*)-**2** and (*P*)-**3** (Figure 4b) and racemic mixtures of **2** and **3** (Figure S15), respectively, can be reasonably explained. On the other hand, if the first cyclization proceeds by the seven-membered ring formation followed by the six- or seven-membered ring formation (Figure S16), the cyclization precursors (*S,S*)- and (*R,R*)-**1** are supposed to be converted to [(*M*)-**2** and (*P*)-**4**] and [(*P*)-**2** and (*M*)-**4**] containing one (**2**) and two (**4**) seven-membered rings, respectively, which were not produced at all. Therefore, this reaction pathway can be completely ruled out.

We next investigated the optical and chiroptical properties of the enantiopure **2** and **3**. The absorption range (< 450 nm) and CD spectral pattern of (*P*)- and (*M*)-**3** were almost identical to those of the pristine [7]helicene (Figure 5b),^[2b] whereas (*P*)- and (*M*)-**2** showed characteristic spectra different from those of the classical aromatic carbohelicenes (Figure 5a).^[19] The absorption edge of **2** (ca. 530 nm) was significantly red-shifted by more than 80 nm compared to those of the pristine [6]helicene (ca. 400 nm)^[2a,19] and **3** (ca. 450 nm) and was even longer than that of the longest carbo[16]helicene (< 500 nm),^[20] although its molar

extinction coefficient (ϵ) above 500 nm was relatively low ($\epsilon < 1000 \text{ M}^{-1}\cdot\text{cm}^{-1}$). The remarkable red-shift in the absorption spectrum of **2** was consistent with the DFT calculations; the HOMO–LUMO gap of **2** (3.17 eV) was narrower than that of **3** (3.76 eV) probably due to the high-lying HOMO level arising from the removal of the degeneracy of the HOMO and HOMO–1 resulting from its nonsymmetric seven-membered ring-embedded helicene skeleton of **2** (Figure S17).^[21]

(*P*)- and (*M*)-**2** showed broad, but perfect mirror-imaged CDs in the absorption region of 250 – 530 nm and the maximum Kuhn's dissymmetry factor ($|g_{\text{abs}}|$) reached 1.5×10^{-2} (505 nm) (Figure 5a), which is higher than those of the pristine [6]helicene ($|g_{\text{abs}}| = 0.92 \times 10^{-2}$)^[19] and (*P*)- and (*M*)-**3** ($|g_{\text{abs}}| = 1.2 \times 10^{-2}$ at 400 nm) (Figure 5b). The CD intensity of (*P*)-**2** in 1,1,2,2-tetrachloroethane remained unchanged at 25 °C after 24 h (Figure S18), but gradually decreased with time at high temperatures (80 – 120 °C) without any change in the absorption spectrum (Figure S19a–c), indicating the dynamic nature of the helicity of **2**. The Gibbs free energy barrier ($\Delta G^{\ddagger}_{298}$) for the racemization of (*P*)-**2** in 1,1,2,2-tetrachloroethane was estimated to be 122 kJ mol^{-1} (Figure S19d), which is in good agreement with that predicted by the DFT calculations ($\Delta G^{\ddagger}_{298} = 117 \text{ kJ mol}^{-1}$) (Figure S20). The helicity inversion barrier of **2** is lower than that of the pristine [6]helicene ($\Delta G^{\ddagger}_{298} = 148 \text{ kJ mol}^{-1}$)^[22] probably because of its structural flexibility due to the nonaromatic seven-membered ring embedded in the helicene framework. The helicity of (*M*)-**3** was

quite stable even at 100 °C as expected from the static nature of the [7]helicene framework (Figure S21).^[22b,23]

The *rac*-**2** and **-3** showed a weak and bright blue photoluminescence (PL) in dichloromethane under irradiation at 365 nm and their quantum yields (Φ_F) were determined to be 3 and 8%, respectively. As expected from the CD and PL performances, the enantiomeric (*P*)- and (*M*)-helicenes showed mirror image CPL spectra in the corresponding fluorescence regions (Figure 5c,d). The maximum luminescence dissymmetry factors ($|g_{lum}|$) of the enantiopure **2** reached ca. 7×10^{-3} that is significantly higher than that of the corresponding [6]helicene (0.9×10^{-3})^[24] as well as that of the (*P*)- and (*M*)-[7]helicene **3** (ca. 3×10^{-3}).

In summary, we have succeeded in the quantitative, stereospecific, and simultaneous synthesis of two enantiopure (>99% ee) (*P*)- and (*M*)-seven-membered ring embedded [6]helicene and carbo[7]helicene from optically-pure doubly axial-chiral *ortho*-phenylene-based cyclization precursors through versatile acid-promoted intramolecular alkyne annulations. The helical handedness of the [6] and [7]helicenes was completely stereo-controlled by the doubly axial chirality of the precursors. The cyclizations proceeded in a stepwise manner; the first hexagonal ring formation followed by the kinetically-controlled heptagonal or hexagonal ring formation with or without helix-inversion of the [4]helicene intermediate, respectively, thus quantitatively producing the enantiopure CPL active [6]- and [7]helicenes with an opposite helicity. The resulting (*P*)- and (*M*)-heptagonal ring-embedded [6]helicenes showed a unique broadband absorption and emission, thereby enabling unexpectedly strong CD and CPL in the long wavelength regions. The $|g_{abs}|$ and $|g_{lum}|$ values reached 1.5×10^{-2} and 7×10^{-3} , respectively, which are greater than those of the corresponding fully aromatic optically-pure [6]helicene and the present [7]helicene.^[19,24] The present findings will provide the potential as a novel methodology for synthesizing a wide variety of enantiopure single and multiple carbo- and heterohelicenes as well as single-handed twisted polycyclic aromatics that will be obtained in a fully stereo-controlled manner when rationally-designed axially chiral multi-biaryl compounds are used as an acid-catalyzed cyclization precursor. In addition, a heptagonal or other unique polygonal ring would be embedded in the helicene framework, leading to further structural and functional diversity in classic yet new helicene chemistry. Work toward these goals is now in progress in our laboratory.

Acknowledgements

We thank Professor Katsuhiko Maeda and Dr. Tatsuya Nishimura (Kanazawa University) for CPL spectral measurements. This work was supported in part by JSPS KAKENHI (Grant-in-Aid for Specially Promoted Research, No. 18H05209 (E.Y. and T.I.) and Grant-in-Aid for Scientific Research (B), No. 21H01984 (T.I.)) and JST PRESTO (No. JPMJPR21A1 (T.I.)).

Keywords: alkyne annulations • chirality transfer • circularly polarized luminescence • seven-membered ring • stereospecific helicene synthesis

- [1] a) R. H. Martin, *Angew. Chem., Int. Ed. Engl.* **1974**, *13*, 649–660; b) W. H. Laarhoven, W. J. C. Prinsen, *Top. Curr. Chem.* **1984**, *125*, 63–130; c) Y. Shen, C.-F. Chen, *Chem. Rev.* **2012**, *112*, 1463–1535; d) M. Gingras, *Chem. Soc. Rev.* **2013**, *42*, 968–1006; e) M. Gingras, G. Félix, R. Peresutti, *Chem. Soc. Rev.* **2013**, *42*, 1007–1050; f) M. Gingras, *Chem. Soc. Rev.* **2013**, *42*, 1051–1095; g) K. Dhbaibi, L. Favereau, J. Crassous, *Chem. Rev.* **2019**, *119*, 8846–8953; h) Y. F. Wu, L. Zhang, Q. Y. Zhang, S. Y. Xie, L. S. Zheng, *Org. Chem. Front.* **2022**, DOI: 10.1039/d1032qo00988a.
- [2] a) M. S. Newman, R. S. Darlak, L. L. Tsai, *J. Am. Chem. Soc.* **1967**, *89*, 6191–6193; b) R. H. Martin, M. J. Marchant, *Tetrahedron* **1974**, *30*, 343–345; c) S. Grimme, J. Harren, A. Sobanski, F. Vögtle, *Eur. J. Org. Chem.* **1998**, *1998*, 1491–1509; d) M. Hasan, V. Borovkov, *Symmetry-Basel* **2018**, *10*, 10; e) F. Pop, N. Zigon, N. Avarvari, *Chem. Rev.* **2019**, *119*, 8435–8478; f) T. Mori, *Chem. Rev.* **2021**, *121*, 2373–2412.
- [3] a) T. Verbiest, S. van Elshocht, M. Kauranen, L. Hellemans, J. Snauwaert, C. Nuckolls, T. J. Katz, A. Persoons, *Science* **1998**, *282*, 913–915; b) R. Kumar, H. Aggarwal, A. Srivastava, *Chem. - Eur. J.* **2020**, *26*, 10653–10675.
- [4] a) V. Kiran, S. P. Mathew, S. R. Cohen, I. H. Delgado, J. Lacour, R. Naaman, *Adv. Mater.* **2016**, *28*, 1957–1962; b) J. R. Brandt, F. Salerno, M. J. Fuchter, *Nat. Rev. Chem.* **2017**, *1*, 0045; c) F. Tani, M. Narita, T. Murafuji, *ChemPlusChem* **2020**, *85*, 2093–2104; d) A. M. Garcia, G. Martínez, A. Ruiz-Carretero, *Front. Chem.* **2021**, *9*, 722727.
- [5] a) H. Tanaka, Y. Inoue, T. Mori, *ChemPhotoChem* **2018**, *2*, 386–402; b) W.-L. Zhao, M. Li, H.-Y. Lu, C.-F. Chen, *Chem. Commun.* **2019**, *55*, 13793–13803.
- [6] a) M. J. Narcis, N. Takenaka, *Eur. J. Org. Chem.* **2014**, *2014*, 21–34; b) P. Aillard, A. Voituriez, A. Marinetti, *Dalton Trans.* **2014**, *43*, 15263–15278; c) C. S. Demmer, A. Voituriez, A. Marinetti, *C. R. Chim.* **2017**, *20*, 860–879; d) J. OuYang, J. Crassous, *Coord. Chem. Rev.* **2018**, *376*, 533–547.
- [7] a) K. Tanaka, Y. Kimura, K. Murayama, *Bull. Chem. Soc. Jpn.* **2015**, *88*, 375–385; b) A. Link, C. Sparr, *Chem. Soc. Rev.* **2018**, *47*, 3804–3815; c) I. G. Stará, I. Starý, *Acc. Chem. Res.* **2020**, *53*, 144–158; d) C. M. Hendrich, K. Sekine, T. Koshikawa, K. Tanaka, A. S. K. Hashmi, *Chem. Rev.* **2021**, *121*, 9113–9163; e) A. Tsurusaki, K. Kamikawa, *Chem. Lett.* **2021**, *50*, 1913–1932.
- [8] A. Urbano, M. C. Carreno, *Org. Biomol. Chem.* **2013**, *11*, 699–708.
- [9] For leading examples of stereospecific synthesis of optically-active carbohelicenes from axially chiral biaryl compounds, see: a) H. J. Bestmann, W. Both, *Angew. Chem., Int. Ed. Engl.* **1972**, *11*, 296; b) I. G. Stará, I. Starý, M. Tichý, J. Závada, V. Hanuš, *J. Am. Chem. Soc.* **1994**, *116*, 5084–5088; c) M. Gingras, F. Dubois, *Tetrahedron Lett.* **1999**, *40*, 1309–1312; d) A. Grandbois, S. K. Collins, *Chem. - Eur. J.* **2008**, *14*, 9323–9329; e) V. Terrasson, M. Roy, S. Moutard, M. P. Lafontaine, G. Pépe, G. Félix, M. Gingras, *RSC Adv.* **2014**, *4*, 32412–32414; f) S. Chen, Z. Ge, Q. Jia, K. P. Wang, L. H. Gan, Z. Q. Hu, *Chem. - Asian J.* **2019**, *14*, 1462–1466; g) U. Dhawa, C. Tian, T. Wdowik, J. C. A. Oliveira, J. Hao, L. Ackermann, *Angew. Chem., Int. Ed.* **2020**, *59*, 13451–13457; h) A. K. Swain, K. Kolanji, C. Stapper, P. Ravat, *Org. Lett.* **2021**, *23*, 1339–1343; i) A. K. Swain, K. Radacki, H. Braunschweig, P. Ravat, *J. Org. Chem.* **2022**, *87*, 993–1000.
- [10] For leading examples of stereospecific synthesis of optically-active heterohelicenes from axially chiral biaryl compounds, see: a) K. Tanaka, H. Suzuki, H. Osuga, *J. Org. Chem.* **1997**, *62*, 4465–4470; b) A. Rajca, M. Miyasaka, M. Pink, H. Wang, S. Rajca, *J. Am. Chem. Soc.* **2004**, *126*, 15211–15222; c) K. Nakano, Y. Hidehira, K. Takahashi, T. Hiyama, K. Nozaki, *Angew. Chem., Int. Ed.* **2005**, *44*, 7136–7138; d) M. Weimar, R. Correa da Costa, F.-H. Lee, M. J. Fuchter, *Org. Lett.* **2013**, *15*, 1706–1709; e) M. Murai, R. Okada, A. Nishiyama, K. Takai, *Org. Lett.* **2016**, *18*, 4380–4383; f) R. Gupta, T. A. Cabrerós, G. Muller, A. V. Bedekar, *Eur. J. Org. Chem.* **2018**, *2018*, 5397–5405; g) M. S. Hossain, M. Akter, M. Shahabuddin, M. Salim, K. Iimura, M. Karikomi, *Synlett* **2022**, *33*, 277–282.
- [11] a) I. R. Márquez, S. Castro-Fernández, A. Millán, A. G. Campaña, *Chem. Commun.* **2018**, *54*, 6705–6718; b) Chaolumen, I. A. Stepek, K. E. Yamada, H. Ito, K. Itami, *Angew. Chem., Int. Ed.* **2021**, *60*, 23508–23532.

-
- [12] For leading examples of carbohelicenes containing one or more seven-membered rings, see: refs 9h, 9i, and a) G. M. Upadhyay, H. R. Talele, A. V. Bedekar, *J. Org. Chem.* **2016**, *81*, 7751–7759; b) X. Li, J. W. Han, Y. X. Zhang, H. N. C. Wong, *Asian J. Org. Chem.* **2017**, *6*, 1876–1884; c) J. Ma, Y. Fu, E. Dmitrieva, F. Liu, H. Komber, F. Hennersdorf, A. A. Popov, J. J. Weigand, J. Liu, X. Feng, *Angew. Chem., Int. Ed.* **2020**, *59*, 5637–5642; d) N. Ogawa, Y. Yamaoka, H. Takikawa, K. Yamada, K. Takasu, *J. Am. Chem. Soc.* **2020**, *142*, 13322–13327; e) Z. Qiu, S. Asako, Y. Hu, C. W. Ju, T. Liu, L. Rondin, D. Schollmeyer, J. S. Lauret, K. Mullen, A. Narita, *J. Am. Chem. Soc.* **2020**, *142*, 14814–14819; f) X. S. Zhang, Y. Y. Huang, J. Zhang, W. Meng, Q. Peng, R. Kong, Z. Xiao, J. Liu, M. Huang, Y. Yi, L. Chen, Q. Fan, G. Lin, Z. Liu, G. Zhang, L. Jiang, D. Zhang, *Angew. Chem., Int. Ed.* **2020**, *59*, 3529–3533; g) K. Kantarod, T. Worakul, D. Soorukram, C. Kuhakarn, V. Reutrakul, P. Surawatanawong, W. Wattanathana, P. Leowanawat, *Org. Chem. Front.* **2021**, *8*, 522–530.
- [13] For pioneering work on an acid-promoted alkyne benzannulation, see: a) M. B. Goldfinger, T. M. Swager, *J. Am. Chem. Soc.* **1994**, *116*, 7895–7896; b) M. B. Goldfinger, K. B. Crawford, T. M. Swager, *J. Am. Chem. Soc.* **1997**, *119*, 4578–4593.
- [14] For leading examples of the quantitative synthesis of defect-free multiple expanded helicenes^[14a] and single-handed helical ladder polymers as well as fully-conjugated ladder polymers^[14b] through a modified acid-promoted alkyne benzannulation that we have recently developed: see: a) W. Zheng, T. Ikai, K. Oki, E. Yashima, *Nat. Sci.* **2022**, *2*, e20210047; b) W. Zheng, T. Ikai, E. Yashima, *Angew. Chem., Int. Ed.* **2021**, *60*, 11294–11299.
- [15] a) P. v. R. Schleyer, C. Maerker, A. Dransfeld, H. Jiao, N. J. R. van Eikema Hommes, *J. Am. Chem. Soc.* **1996**, *118*, 6317–6318; b) Z. Chen, C. S. Wannere, C. Corminboeuf, R. Puchta, P. v. R. Schleyer, *Chem. Rev.* **2005**, *105*, 3842–3888.
- [16] E. González-Fernández, L. D. M. Nicholls, L. D. Schaaf, C. Farès, C. W. Lehmann, M. Alcarazo, *J. Am. Chem. Soc.* **2017**, *139*, 1428–1431.
- [17] S. Jia, S. Li, Y. Liu, W. Qin, H. Yan, *Angew. Chem., Int. Ed.* **2019**, *58*, 18496–18501.
- [18] Yan et al. demonstrated that the axially chiral biaryl units generated during the first alkyne benzannulation catalyzed by chiral organocatalysts contributed to the subsequent diastereoselective [6]helicene formation, which, however, proceeded mostly under chiral catalyst control, see ref 17.
- [19] Y. Nakai, T. Mori, Y. Inoue, *J. Phys. Chem. A* **2012**, *116*, 7372–7385.
- [20] K. Mori, T. Murase, M. Fujita, *Angew. Chem., Int. Ed.* **2015**, *54*, 6847–6851.
- [21] Such a red-shift was not observed for pyrene-fused [5]- and [7]helicenes connected via a seven-membered ring when compared to the corresponding carbohelicenes, see refs 9h and 9i.
- [22] a) R. H. Martin, M.-J. Marchant, *Tetrahedron Lett.* **1972**, *13*, 3707–3708; b) P. Ravat, *Chem. - Eur. J.* **2021**, *27*, 3957–3967.
- [23] R. H. Martin, M. J. Marchant, *Tetrahedron* **1974**, *30*, 347–349.
- [24] H. Tanaka, M. Ikenosako, Y. Kato, M. Fujiki, Y. Inoue, T. Mori, *Comm. Chem.* **2018**, *1*, 38.